



LUND UNIVERSITY

Investigation and compensation of the nonlinear response in photomultiplier tubes for quantitative single-shot measurements.

Knappe, Christoph; Lindén, Johannes; Abou Nada, Fahd Jouda; Richter, Mattias; Aldén, Marcus

Published in:
Review of Scientific Instruments

DOI:
[10.1063/1.3693618](https://doi.org/10.1063/1.3693618)

2012

[Link to publication](#)

Citation for published version (APA):

Knappe, C., Lindén, J., Abou Nada, F. J., Richter, M., & Aldén, M. (2012). Investigation and compensation of the nonlinear response in photomultiplier tubes for quantitative single-shot measurements. *Review of Scientific Instruments*, 83(3), [034901]. <https://doi.org/10.1063/1.3693618>

Total number of authors:
5

General rights

Unless other specific re-use rights are stated the following general rights apply:

Copyright and moral rights for the publications made accessible in the public portal are retained by the authors and/or other copyright owners and it is a condition of accessing publications that users recognise and abide by the legal requirements associated with these rights.

- Users may download and print one copy of any publication from the public portal for the purpose of private study or research.
- You may not further distribute the material or use it for any profit-making activity or commercial gain
- You may freely distribute the URL identifying the publication in the public portal

Read more about Creative commons licenses: <https://creativecommons.org/licenses/>

Take down policy

If you believe that this document breaches copyright please contact us providing details, and we will remove access to the work immediately and investigate your claim.

LUND UNIVERSITY

PO Box 117
221 00 Lund
+46 46-222 00 00

Investigation and compensation of the nonlinear response in photomultiplier tubes for quantitative single-shot measurements

C. Knappe, J. Lindén, F. Abou Nada, M. Richter, and M. Aldén

Citation: [Rev. Sci. Instrum.](#) **83**, 034901 (2012); doi: 10.1063/1.3693618

View online: <http://dx.doi.org/10.1063/1.3693618>

View Table of Contents: <http://rsi.aip.org/resource/1/RSINAK/v83/i3>

Published by the [American Institute of Physics](#).

Related Articles

Short wavelength thermography: Theoretical and experimental estimation of the optimal working wavelength
[J. Appl. Phys.](#) **111**, 084903 (2012)

Hole shape effect induced optical response to permittivity change in palladium sub-wavelength hole arrays upon hydrogen exposure
[J. Appl. Phys.](#) **111**, 084502 (2012)

Few-photon-level two-dimensional infrared imaging by coincidence frequency upconversion
[Appl. Phys. Lett.](#) **100**, 151102 (2012)

A readout for large arrays of microwave kinetic inductance detectors
[Rev. Sci. Instrum.](#) **83**, 044702 (2012)

Channelling optics for high quality imaging of sensory hair
[Rev. Sci. Instrum.](#) **83**, 045001 (2012)

Additional information on Rev. Sci. Instrum.

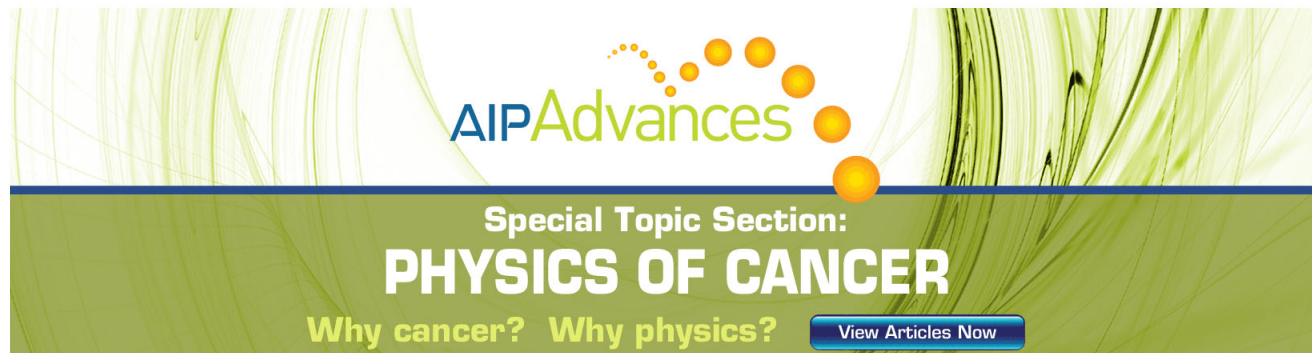
Journal Homepage: <http://rsi.aip.org>

Journal Information: http://rsi.aip.org/about/about_the_journal

Top downloads: http://rsi.aip.org/features/most_downloaded

Information for Authors: <http://rsi.aip.org/authors>

ADVERTISEMENT

The advertisement features a green and yellow abstract background with flowing lines. At the top, the 'AIP Advances' logo is displayed, with 'AIP' in blue and 'Advances' in green, accompanied by a series of orange dots of varying sizes. Below this, the text 'Special Topic Section: PHYSICS OF CANCER' is written in white, with 'PHYSICS OF CANCER' in a larger, bold font. At the bottom, the phrase 'Why cancer? Why physics?' is written in yellow, and a blue button with the text 'View Articles Now' is positioned on the right.

AIP Advances

Special Topic Section:
PHYSICS OF CANCER

Why cancer? Why physics? [View Articles Now](#)

Investigation and compensation of the nonlinear response in photomultiplier tubes for quantitative single-shot measurements

C. Knappe, J. Lindén, F. Abou Nada, M. Richter, and M. Aldén

Division of Combustion Physics, Lund University, Box 118, SE-221 00 Lund, Sweden

(Received 6 December 2011; accepted 23 February 2012; published online 15 March 2012)

A concept for time-sensitive optical detectors is described that shows how to confirm whether the detection device is operating in the linear response regime. By evaluating the recorded time decay of a thermographic phosphor, even weak saturation effects far from obvious situations can be identified and further related to either optical or electrical saturation. The concept has been validated by running a PMT detector close to saturation and exposing it to the optical signal decay of two different thermographic phosphors, $\text{La}_2\text{O}_2\text{S:Eu}$ and CdWO_4 . It was confirmed that short but intense light exposures at the beginning of an individual time decay influence the detector response for the rest of the decaying signal including temporal areas, where the anode current has dropped well below the manufacturer specified current limit. Such situations are common when applying, e.g., phosphor thermometry where it is necessary to retrieve the full decay curve from a single-shot event, i.e., standard techniques based on single-photon counting are omitted. Finally, means of compensation are introduced in order to facilitate the retrieval of useful information from the measurement data when operation in the non-linear response regime is inevitable. © 2012 American Institute of Physics. [<http://dx.doi.org/10.1063/1.3693618>]

I. INTRODUCTION

The purpose of an optical detector is to convert incoming light into a measurable signal, principally electronic, which is proportional to the light intensity. While there are many different types of detectors, all are applied in one of two ways: to reproduce light intensity in a temporally resolved manner, e.g., photodiodes or photomultiplier tubes (PMTs); to integrate the light intensity over time, e.g., CCD detectors. Both applications can be used for quantitative measurements, providing that the signal response is linear (linear response region), or that corrections can be made when the input-to-output signal is nonlinear. The linear response region for detectors is often defined relative to the noise threshold and a maximum value such as anode current or digitizer limit; however, in practice, saturation effects can be seen at values much lower than these perceived extrema.

When measuring phosphorescence decay times with a PMT, for investigation of phosphor thermometry, it was found that the photomultiplier settings for gain and exposure level were linked to variations in the measured decay time, though levels were below the proscribed limits. This behavior was consistent with saturation phenomena. The purpose of this paper is to present a simple method to determine the true linear response region for any temporally resolved optical detector, as well as presenting a method to correct measurements outside the linear response region. For consideration of similar effects in integrating optical detectors see Ref. 1, where an image intensified CCD is investigated.

Photomultiplier tubes are perhaps the most widely used electronic tool in spectroscopy, having been applied in every manner of optical measurement.²⁻⁴ The PMT provides opto-electrical conversion combined with internal electrical amplification, see Figure 1, making it suitable for low light

level measurements. They are temporally resolved detectors; depending on circuitry they can resolve, in real time, the impingement of single photons on the detector, or measure continuous streams of photons. It is the ability of a PMT to operate continuously that is used in phosphor thermometry to measure the temperature dependent phosphorescence decay. For a more in-depth description of the working principles of a PMT, see Hakamata *et al.*⁵ For a detailed model of photomultiplier gain, see Moatti.⁶

Significant efforts have been made to characterize nonlinearity in PMTs thus far. Sauerbrey,⁷ for example, published a substantial experimental study of PMT nonlinearity in which five essentially independent sources of photomultiplier nonlinearity were measured. According to Ref. 7 some sources of PMT nonlinearity can be easily avoided as they are introduced by external circuitry connected to the PMT. Complementary to Sauerbrey's work, Aspnes and Studna⁸ designed a circuit for improving photomultiplier linearity. More recent work dealt with the calibration of non-linear photomultiplier response. In 2003, Vicić *et al.*⁹ used an ultraviolet pulsed-light source and determined the response of a photomultiplier within a range of light intensities from single photoelectrons up to well beyond the linear response region. Whilst

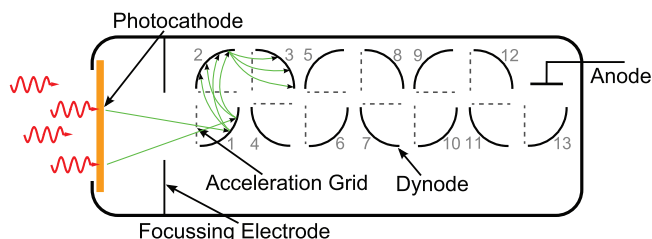


FIG. 1. Schematic construction of a PMT with 13 dynodes.

maintaining an “excellent agreement” between their measured data and the fitted model, Vičić admitted that the procedure described in Ref. 9 was “extremely computer-intensive.”

It is not in the scope of this paper to present yet another in-depth discussion of PMT physics; rather, a rapid and easily accessible tool is constructed to properly evaluate the operating region of the PMT. To this end, a simple view of PMT behavior was adopted for temporally resolved, non-photon-counting instances. Ideally, the PMT response is a linear relationship between photon flux and output current. The linear response is susceptible to two independent processes that drive the PMT into the nonlinear response region when approaching saturation.¹⁰

The first process, photocathode bleaching, occurs when the photocathode is struck by a sufficient number of photons per time interval to deplete the valence band in the photocathode. A radial voltage drop at the photocathode is caused by large current densities and a certain time is needed for the photocathode to recover and re-enter the linear response region.

The accumulation of local electric fields inside the PMT accounts for the second process. At high gains, a space charge builds at the anode and last few dynode stages. This space charge electrically shields and decelerates advancing electrons. Hence, increasing electrical gain above a certain threshold drives the dynode chain into the saturated region. This is often considered as the major source of saturation in PMTs.¹¹

The total detector response, can be understood as the product of the optical- (photocathode) and the electrical (dynode chain) response functions. These processes are not discrete, as the number of electrons arriving at the anode, and thus gain saturation, depends on the photocathode sensitivity and the amount of incoming light. Alternatively, reducing incoming light intensities will suppress the development of a space charge (as does lowering gain or applying a higher voltage across the last few dynodes). As a result, uncorrected quantitative measurements can only be performed if the PMT is operated in the linear region for both of these two responses.

Most PMTs are specified to run at a maximum DC output current of 100 μA ,^{5,12} which equals approximately 6×10^5 electrons/ns released at the last dynode. This current value can be understood as the absolute limit for linear dynode operation, though the photocathode may already be saturated due to the incoming light flux. According to Becker and Hickl,¹³ this maximum output current can be increased almost by a factor of 1000 to around 100 mA when operating in the PMT in “pulsed” mode, mostly because the PMT can recover, to some extent, from bleaching and space charge accumulation in between two adjacent pulses.

A motivation for extending the output current beyond 100 μA is to increase the output signal: most PMTs come with a load resistance of 50 Ω , meaning that the readout instrument’s input resistance has to match in order to avoid back and forth reflection (“ringing”) of the signal in the cable. By Ohm’s law, a current of 100 μA over 50 Ω generates a maximum voltage of 5 mV, close to the lower resolution limit of common digital oscilloscopes. This often results in unacceptably low signal/noise ratios when digitizing the analog current, without time averaging or special amplification electron-

ics. When approaching pulse lengths of as much as a few milliseconds, as in some cases of phosphorescence, it is dubious that these enhanced limits still apply, and caution should be exercised when extending the PMT workspace by exceeding the anode’s current limit.

II. DATA ACQUISITION AND EVALUATION

Temporally, resolved intensity decay curves were acquired for two different phosphors ($\text{La}_2\text{O}_2\text{S:Eu}$ with 2 at. % Eu and CdWO_4) in order to generate different optical intensity time-distributions that the detector has to reproduce. The major difference between these two phosphors is an intense, short-lived, fluorescence peak, that is present for the $\text{La}_2\text{O}_2\text{S:Eu}$, but is missing in the CdWO_4 time decay (see Figure 2).

Each phosphor was excited by a 10 Hz pulsed, Q-switched and frequency tripled (355 nm, $\text{La}_2\text{O}_2\text{S:Eu}$) or frequency quadrupled (266 nm, CdWO_4) Nd:YAG laser (Quantel Brilliant B). Low laser pulse energies between 70 and 140 μJ were used in order to avoid saturating the phosphor. The resulting phosphorescence was imaged onto a photomultiplier module (Hamamatsu H6780-04) after passing an interference filter, centered at 540 nm (FWHM = 10 nm) for the $\text{La}_2\text{O}_2\text{S:Eu}$ phosphor and 450 nm for CdWO_4 (FWHM = 40 nm). The filters were placed in front of the detector to eliminate spurious laser radiation and to spectrally isolate the phosphorescence emission.

In the PMT, a nominal electrical gain can be chosen within the range of 10^2 to 10^6 (Ref. 12), depending on the amount of optical signal that is available for collection. The gain number is defined by the ratio of output electrons divided by photocathode electrons. The photomultiplier output current was read out by a 350 MHz digital oscilloscope (Lecroy WaveRunner WA6030) at an input resistance of 50 Ω , allowing sampling of decay times as short as a few ns at a dynamic range of 8 bit.

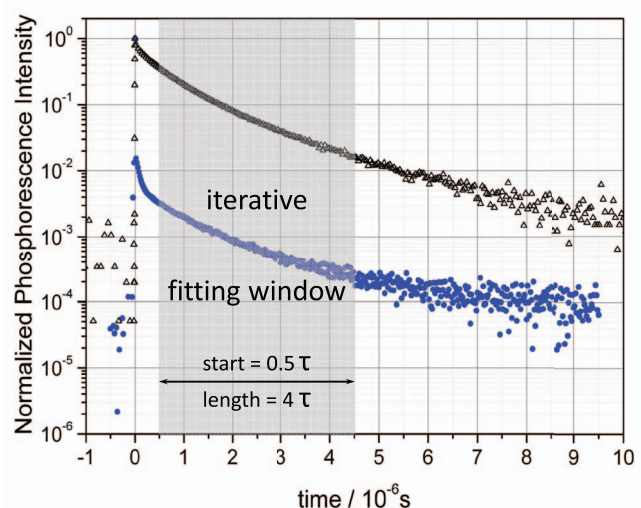


FIG. 2. A comparison of similar phosphorescence decays for $\text{La}_2\text{O}_2\text{S:Eu}$ (at 540 nm, $T = 518$ K blue dots) and CdWO_4 (at 450 nm, $T = 387$ K, black triangles). The gray area indicates the time window in which the decay time is determined.

Both phosphors offer emission peaks that decay exponentially after laser excitation. The time decay can be approximated by

$$I = I_0 \cdot \exp\left(-\frac{t}{\tau}\right), \quad (1)$$

where I_0 is the initial emission intensity, t is time and τ is the decay time of the phosphorescence, i.e., the time after which the intensity has decreased to $1/e$ of the initial emission I_0 .

To extract the time constant τ from the measured decay curves, a Levenberg-Marquard fitting algorithm (MATLAB) has been applied, that varies I_0 and τ and iteratively adapts the $(n+1)$ th fitting window region according to the n th evaluated decay time τ_n until stability is achieved. As indicated in Figure 2 (grayed out), the fitting window was chosen to range from $0.5\tau_n$ to $4.5\tau_n$. Further details on the iterative decay time algorithm can be found in Ref. 14.

For obvious reasons, the recorded phosphorescence decay time τ is a measure of the time-distribution of the detector output signal $S_{\text{out}}(t)$. Therefore, τ is also a suitable target for analyzing the linearity of a detector's input-to-output signal conversion. In other words, the detector operates in the linear region when the evaluated decay time is purely dependent on the light source and thus insusceptible to minor changes regarding detector gain and light exposure. Consequently, the detector linearity can be analyzed either by changing the electrical amplification (gain) or by attenuating the light before it hits the detector. In case of linear operation the evaluated decay time will be constant, regardless these changes that were made on the detector side.

In a simplified approach that emphasizes how detector saturation distorts the output signal, detector response functions were simulated according to

$$S_{\text{out}}(I_{\text{in}}) = S_{\text{max}} \cdot \left[1 - \exp\left(-\frac{I_{\text{in}}}{S_{\text{max}}}\right) \right] \quad (2)$$

where I_{in} is the incoming signal intensity and S_{max} is the maximum signal output intensity. Such response curves were plotted in Figure 3(a) together with the response curve of an ideal detector indicated by the black solid line. By inserting a phosphorescence intensity distribution as I_{in} into equation (2), a distorted detector output signal can be obtained, which is shown in part (b) of Figure 3 for each corresponding response curve from Fig. 3(a). A least squares exponential fit according to equation (1) was performed within the indicated time window illustrated in grey. The graph in Figure 3(c) displays the associated decay times, which clearly depend on the saturation level, that was defined by how much the initial output (see Fig. 3(b), black curve) signal was reduced due to detector saturation in percentage.

As displayed in Figure 4, the time decays of CdWO_4 and $\text{La}_2\text{O}_2\text{S:Eu}$ exhibit a strong temperature dependence between 300 K and 600 K, which makes them a sensitive remote temperature sensor, for example in engine applications.^{4,15,16}

Both phosphors combined have a common range of decay times from 10 μs down to 100 ns. This broad overlap region is beneficial as it allows achieving similar decay times by keeping the two phosphors at different temperatures. This

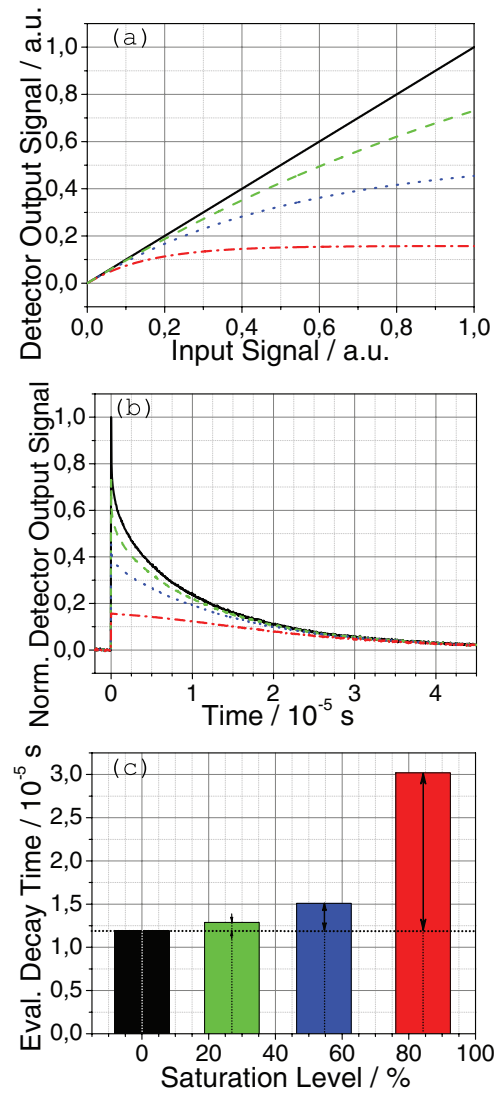


FIG. 3. Example on how different saturation states in the detector (a) change the shape of the output time-signal (b) and the evaluated decay time (c). The time decay in black corresponds to an average of 100 measured decay curves from $\text{La}_2\text{O}_2\text{S:Eu}$ at room temperature.

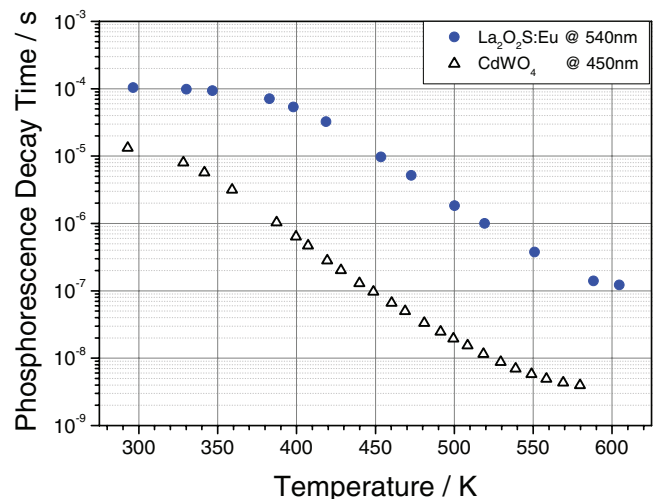


FIG. 4. Phosphorescence decay time as function of temperature for $\text{La}_2\text{O}_2\text{S:Eu}$ and CdWO_4 .

in turn enables the impact of an intense initial peak (present for $\text{La}_2\text{O}_2\text{S:Eu}$, absent for CdWO_4) on the detector response to be studied by comparison under otherwise similar operating conditions.

III. RESULTS

A. Saturation analysis using phosphorescence time decay

For 100 consecutive laser shots at room temperature, the $\text{La}_2\text{O}_2\text{S:Eu}$ phosphorescence decay time τ is displayed in Figure 5(a). At a PMT gain of 4700 and mean laser pulse energy of $70 \mu\text{J}$, the spread in phosphorescence decay time ranges from $103.5 \mu\text{s}$ to $104.2 \mu\text{s}$. According to the measurement data displayed in Figure 4, the spread corresponds to a temperature interval from 294 K to 299 K. What initially looks like a statistical distribution due to noise in the signal or temperature variation (see Figure 5(a)) becomes a linear trend when the measurement points are re-arranged according to the output signal voltage $S_{\text{out}}(t = 0.5\tau)$, see Figure 5(b). $S_{\text{out}}(t = 0.5\tau)$ is equal to the very first readout voltage within

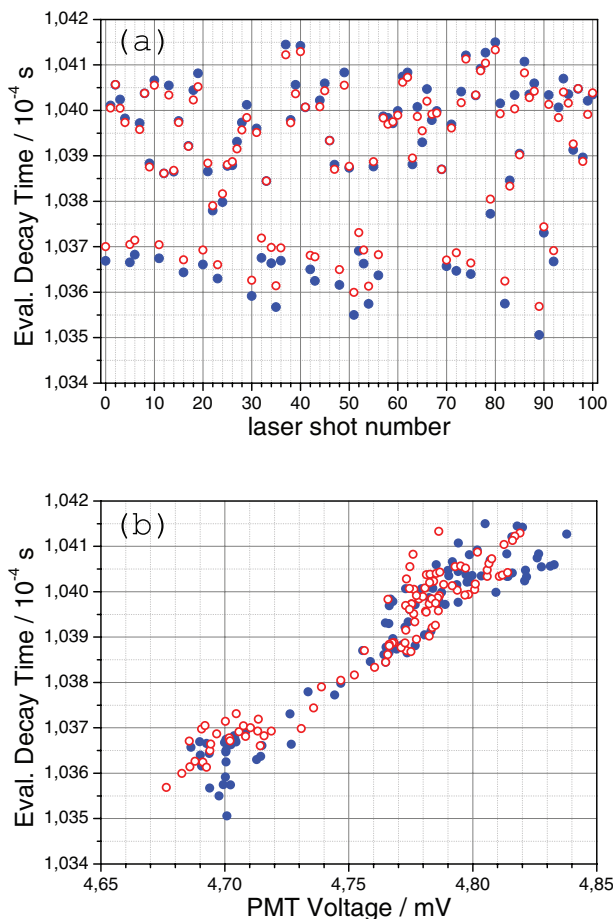


FIG. 5. $\text{La}_2\text{O}_2\text{S:Eu}$ phosphorescence decay time at 296 K using gain 4700 and 100 consecutive laser shots at $\sim 70 \mu\text{J}$ (a). In graph (b), the same data has been re-arranged according to the first output voltage within the fitting window $S_{\text{out}}(t = 0.5\tau)$. Blue dots represent decay times obtained by using an iteratively changing time window (see Ref. 14) whereas the red circles illustrate the same data evaluated in a fixed time window.

the fitting window, see Figure 2 for an example. Its average value is 4.75 mV, which corresponds to $95 \mu\text{A}$ in PMT output current at 50Ω oscilloscope input resistance. The spread in voltage is about 3 % and corresponds to laser energy shot-to-shot variations that induced proportionally shifting phosphorescence yields. According to Ref. 12, an output current of $95 \mu\text{A}$ is still below the $100 \mu\text{A}$ specified limit of the cw PMT operation. However only half a decay time earlier (see Figure 2), where the phosphorescence signal coincides with spurious laser reflexes, i.e., $52 \mu\text{s}$ prior to the fitting window start position, the PMT was struck by far more photons, corresponding to 20 mA PMT output current (not shown in Figure 5) which is 200 times higher than the specified cw limit, but still only about 1/5 of what would be the limit for pulsed operation according to Ref. 13.

The results from Figure 5 are obtained taking two different approaches: An iteratively changing fitting window that adapts its size and position according to the length of each individual decay curve (red circles) and a fixed time window for all curves, which was determined by the average iterative fitting window (blue dots). As can be seen in Figure 5, the method of data reduction has an influence on its own upon the obtained results. Similarly, it can be shown that even low level spurious background radiation can have an effect on measurement accuracy. However, being able to reproduce the intensity dependence of τ with a fixed time window is an evidence for a physical change in decay time, showing that these effects are not simply induced by evaluating different time windows. Even though the results in Figure 5(b) overlap quite nicely, the slope for the iterative time window (blue dots) is a little higher accounting for the slight differences in the window positions: Due to the slight multi-exponential time decay that characterizes phosphorescence emitted by $\text{La}_2\text{O}_2\text{S:Eu}$ (see Figure 2), a decay time evaluated in an earlier part of the curve results in a smaller value compared to a decay time evaluated slightly later in the same curve. In summary, the trends shown in Figure 5 can clearly be interpreted as a distortion of the temporal signal shape that correlates with the amount of light hitting the PMT. The different intensities were induced by laser shot-to-shot variations and cannot be avoided, which makes this dependence a concern for any quantitative, time dependent optical measurement involving lasers. The positive slope is in agreement with what would be expected from a saturation effect (see Figure 3). However, it remains yet unclear, whether the saturation was caused by photocathode bleaching and/or by applying too high electrical amplification.

For investigating the source of saturation further, Figure 6 displays two measurement series of time decays, taken at 382 K, this time using two different gains (4700 and 7400) at constant mean laser energy of $70 \mu\text{J}$.

The two point clusters shown in Figure 6 correspond to the lower gain value (left) and the higher gain (right), and incorporate a series of 100 laser shots each, represented by the spread in x-direction. For a linear responding detector, the two point clusters in Figure 6 were expected to collapse in y-direction into one single decay time. Hence, PMT saturation shows its effect by linearly distributing the decay times as a function of PMT output

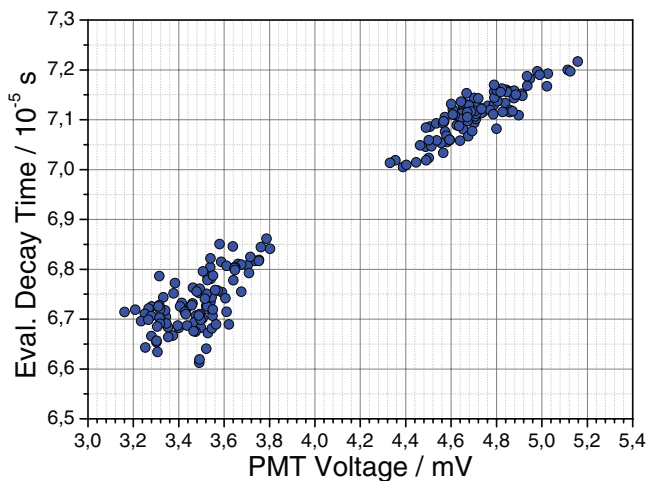


FIG. 6. $\text{La}_2\text{O}_2\text{S:Eu}$ phosphorescence decay times at 382 K using two gains, 4700 (left group) and 7400 (right group) with 100 consecutive laser shots at $\sim 70 \mu\text{J}$ each. The data has been plotted as a function of the PMT Voltage $S_{\text{out}}(t = 0.5\tau)$.

voltage. An interesting observation is that both clusters are positioned to each other such that the individual slope from each gain measurement matches the other data cluster. In other words, the slope caused by variation from the photocathode's amount of primary electrons (shot-to-shot based) is identical to the cluster offset slope that is caused by elevating the gain. From these observations it is possible to conclude the following:

1. Since both point clusters show a non-constant decay time distribution – both gain measurement are subject to a nonlinear detector response.
2. The gain-driven cluster offset indicates electrical saturation: If the slope within each cluster was only due to photocathode saturation – the second point cluster would result in similar decay times obtained at higher output voltages, i.e., a cluster offset parallel to the x-direction.
3. The saturation seen in Figure 6 is purely gain-driven with no significant contributions of photocathode saturation, meaning that if the number of primary photoelectrons would be increased, the decay curve shape would change the same way as if the gain is increased. If also the photocathode was subject to saturation, the individual point cluster slopes would not match the gain-based cluster offset slope.

Figure 7 shows data that is similar to those that was presented in Figure 6, only this time at an elevated temperature of 519 K. The laser energy was kept low again to $70 \mu\text{J}$ and two gain values are compared to each other (4700 and 8400).

From a comparison with Figure 6 the cluster offset slope is a factor of 84 smaller in Figure 7. Also, the relative decay time spread in each measurement increased as shorter decay times become more difficult to evaluate. Since the phosphorescence intensity decreases towards higher temperatures, the PMT voltage at gain 4700 for 382 K (see Figure 6) is almost twice as high as for 519 K (see Figure 7) for the same mean laser pulse energy. Additionally, the decay time at

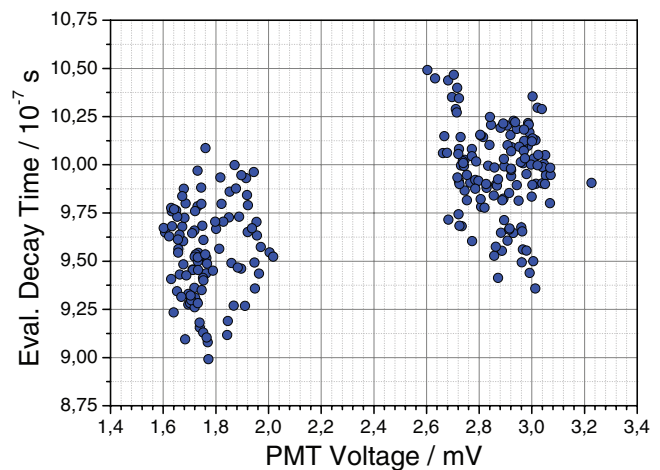


FIG. 7. $\text{La}_2\text{O}_2\text{S:Eu}$ phosphorescence decay times at 519 K using two gains, 4700 (left) and 8400 (right), with 100 consecutive laser shots at $\sim 70 \mu\text{J}$ each.

519 K was 71 times shorter than for 382 K in Figure 6, reducing the mean light exposure time. Therefore less load was put on the dynode chain, which could explain the reduced cluster offset slope, seen in Figure 7.

B. Compensation approach

Operating outside the linear workspace of a detector is often required due to the higher signal intensity available. However, the distortions in the response signal due to saturation are a source of systematic error. Nevertheless, a compensation that accounts and corrects for these effects is possible, providing systematic changes in the response are mapped into a library and thus can be sufficiently predicted. In practice, a biased result originating from a slightly saturated signal can be transformed into an unbiased result by extrapolating it towards lower signal levels into the linear operating region, using a slope proposed by the detector library. For probe techniques that rely on calibration rather than an absolute physical quantity, such as thermographic phosphorescence, the compensation is simplified because the reference is not restricted to the linear detector operating region: Any signal output can become a reference for extrapolation. For further considerations, the reference was chosen as the PMT-readout voltage $S_r(t = 0.5\tau)$ recorded over 50Ω .

The upper part (a) of Figure 8 shows the PMT decay response slope $d\tau/dS$ for $\text{La}_2\text{O}_2\text{S:Eu}$ decays as a function phosphorescence decay time (red circles). In graph (b) on the bottom of Figure 8, $d\tau/dS$ is presented in red as a function of temperature together with corresponding decay time values (blue dots) that were taken from the calibration curve in Figure 4. The spline interpolation (red dashed line) can be used to correct decay times obtained in the nonlinear detector regime. It refers to an output reference voltage of $S_r(t = 0.5\tau) = 4.8 \text{ mV}$ at the start of the decay window, for which the calibration was performed.

As the comparison between Figure 6 and 7 suggested, the slope declines for shorter time decays, probably due to the competition between saturation and space charge recovery that was briefly discussed above. The spline interpolation

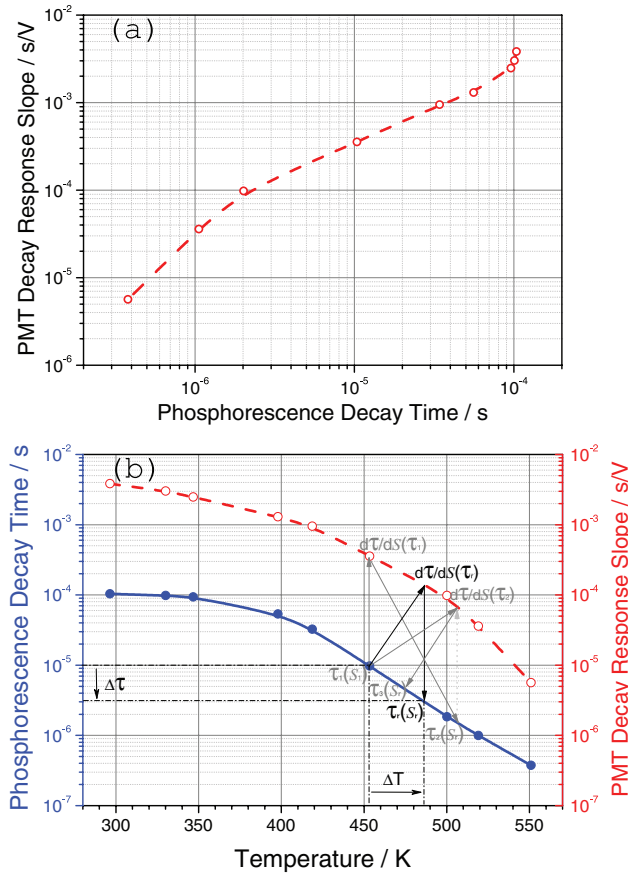


FIG. 8. PMT decay response slope for $\text{La}_2\text{O}_2\text{S:Eu}$ (red circles) as a function of phosphorescence decay time (a) and as a function of temperature (b). The black arrows in graph (b) indicate how a measured decay time $\tau_1(S_1)$ can be iteratively corrected towards τ_r at reference signal output S_r ($< S_1$) for which the phosphor was calibrated (blue dots).

indicated in red, can further be used for compensating any obtained decay time towards the reference output voltage of $S_r(t = 0.5\tau) = 4.8$ mV, which refers to the first output voltage within the decay evaluation window. Knowing how detector distorted decay times evolve, the correction of τ_1 recorded at a output voltage of $S_1(t = 0.5\tau)$ can be performed to the reference value τ_r at reference voltage S_n according to equation (3),

$$\tau_r = \tau_1 - \left. \frac{d\tau}{dS} \right|_{\tau_r} \cdot (S_1 - S_r). \quad (3)$$

Although $d\tau/dS(\tau_r)$ is initially unknown because it requires knowledge over τ_r , it can be approached iteratively by starting with $d\tau/dS(\tau_1)$. For $d\tau/dS > 0$ and $S_1 > S_r$ it follows that $\tau_1 > \tau_r$ and $d\tau/dS(\tau_1) > d\tau/dS(\tau_r)$ as seen in Figure 8(b), meaning that the first iteration $\tau_2(S_r)$ will underestimate τ_r when correcting from S_1 against S_r . In a second iteration step, the slope $d\tau/dS(\tau_2) < d\tau/dS(\tau_r)$ can be used to correct $\tau_1(S_1)$ towards $\tau_3(S_r) < \tau_1(S_1)$, which in term is an overestimation of τ_r . Since τ_3 already is a closer estimate of τ_r compared to τ_1 , the iterative solution converges oscillating towards τ_r , granted that $d\tau/dS$ is monotonic. Considering $d\tau/dS > 0$ and signal intensities smaller than the reference, i.e., $S_1 < S_r$, a similar

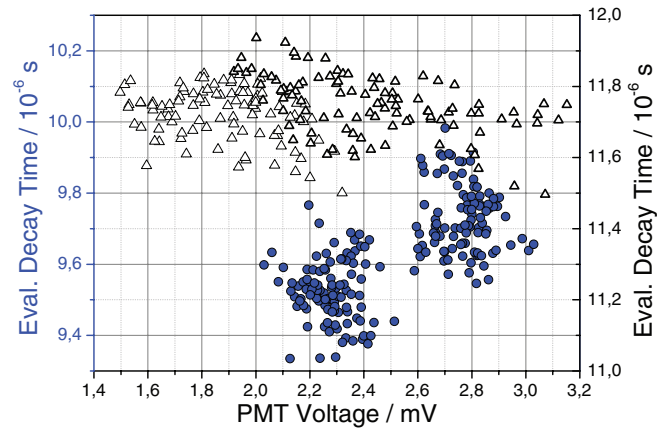


FIG. 9. Comparison of response slopes for two different phosphors (blue dots: $\text{La}_2\text{O}_2\text{S:Eu}$ at 473 K; black triangles: CdWO_4 at 308 K) at similar decay times, using equal PMT gains (4700 and 6300) and laser energies that yield the same decay signal values.

argumentation results in τ_i converging towards $\tau_r > \tau_1$, however this time without oscillations. In summary, if measurements of a certain decay time are taken at output voltages S_1 different from the reference signal S_r for which the calibration $d\tau/dS$ (see Figure 8) was performed, the decay time has first to be corrected towards that reference signal intensity before the decay time can be converted into a temperature.

It is, however, important that the PMT is corrected for the same type of signal/phosphor, as indicated by the earlier assumption that the detector might be affected by pre-existing saturation states. To test this hypothesis, the PMT was now used to detect similar time decays from $\text{La}_2\text{O}_2\text{S:Eu}$ and CdWO_4 at laser energies adjusted to generate the same output current for both signals within the investigated time window. Since the gain was identical in both cases, the laser energy was adapted to compensate for the two different phosphorescence yields and to account for the spectral photocathode sensitivity within the corresponding emission wavelengths such that the same amount of primary electrons were released from the photocathode. The experiment is set up in a way that an ideal time gated PMT, switched on only during the evaluated time window, should have no means to distinguish the two different phosphorescence emissions. However the PMT used here also recorded a peak voltage prior to the evaluation window, that was about 54 times higher for the $\text{La}_2\text{O}_2\text{S:Eu}$ phosphor than for CdWO_4 . In Figure 9, the results for the two cases are displayed, showing a horizontal response distribution for CdWO_4 in contrast to the results obtained with $\text{La}_2\text{O}_2\text{S:Eu}$. The bigger spread in PMT voltage for CdWO_4 is due the higher signal yield for CdWO_4 that required less, and thus more unstable, laser excitation energy.

According to Figure 9, the decay time slope has drastically changed by the presence of the peak prior to the fitting window in which the decay time was evaluated. It can thus be concluded that strong and saturating peaks in the beginning have an impact on the time progression of the detected signal. As long as these peaks cannot be avoided by some sort of time-gating, detector compensation should also take into account the time dependent photon emission curve of the light source that is to be investigated.

IV. CONCLUSIONS

In this paper, a novel test procedure is described that can be used to determine the linear operating region of any optical detector, capable of performing time-resolved measurements. Additionally, information is provided on how such a detector can be operated outside the linear regime as is often required when signal decay time information must be retrieved from single-shot measurements. The procedure was applied to the extended afterglow of thermographic phosphors and compares evaluated signal decay times as a function of electrical gain and incident intensity by creating a detector response database. By evaluating and comparing the recorded time decay within the response database even weak saturation effects (far from obvious situations) can be identified and further related to either photocathode or dynode saturation.

These saturation events introduce a systematic error on quantitative measurements results. Such errors can be corrected towards a reference value from the detector's response database. The reference value needs to be part of the linear response regime in most cases. However, if the reference value is used only to calibrate another quantity – as it is for phosphor thermometry – any value from the detector response database can be chosen as a reference.

Furthermore, a comparison of the decay signals from CdWO_4 and $\text{La}_2\text{O}_2\text{S:Eu}$ has shown that an accurate correction for PMT non-linearity should also consider the history of the signal, e.g., the photo-current at the start of the decay. It is thus important from a compensation point of view to use the same sort of signal for both, the actual measurement and the generation of the response database.

ACKNOWLEDGMENTS

This work was financially supported by the HELIOS research project within the 7th EU framework program for Research and Technical Development/Transportation and the research project D60, financed by the Swedish Energy Agency. The authors gratefully acknowledge A. W. Sloman for helpful discussions.

- ¹J. Lindén, C. Knappe, M. Richter, and M. Aldén, *Meas. Sci. Technol.* **23**, 035201 (2012).
- ²M. P. Bristow, *Appl. Opt.* **37**, 6468 (1997).
- ³H. Bladh, J. Johnsson, and P. E. Bengtsson, *Appl. Phys. B* **96**, 645 (2009).
- ⁴C. Knappe, P. Andersson, M. Algotsson, M. Richter, J. Lindén, M. Tunér, B. Johansson, and M. Aldén, *SAE Int. J. Engines* **4**, 1689 (2011).
- ⁵T. Hakamata, H. Kume, K. Okano, K. Tomiyama, A. Kamiya, Y. Yoshizawa, H. Matsui, I. Otsu, T. Taguchi, Y. Kawai, H. Yamaguchi, K. Suzuki, S. Suzuki, T. Morita, and D. Uchizono, *Photomultiplier Tubes – Basics and Applications* (Hamamatsu Photonics K.K., Iwata City, 2007).
- ⁶P. Moatti, *L'Onde Electrique* **43**, 787 (1963).
- ⁷G. Sauerbrey, *Appl. Opt.* **11**, 2576 (1972).
- ⁸D. E. Aspnes and A. A. Studna, *Rev. Sci. Instrum.* **49**, 291 (1978).
- ⁹M. Vikić, L. G. Sobotka, J. F. Williamson, R. J. Charity, and J. M. Elson, *Nucl. Instrum. Methods A* **507**, 636 (2003).
- ¹⁰D. H. Hartman, *Rev. Sc. Instrum.* **49**, 1130 (1978).
- ¹¹H. Kunz, *Metrologia* **5**, 88 (1969).
- ¹²H6780-04 PMT Datasheet, http://sales.hamamatsu.com/assets/pdf/parts_H/H6780-04.pdf.
- ¹³W. Becker and H. Hickl, *How (and why not) to Amplify PMT Signals* (Becker & Hickl GmbH, Berlin, 2000), <http://www.becker-hickl.de/pdf/ampmt.pdf>.
- ¹⁴J. Brübach, J. Janicka, and A. Dreizler, *Opt. Las. Eng.* **47**, 75 (2009).
- ¹⁵G. Särner, M. Richter, and M. Aldén, *Meas. Sci. Technol.* **19**(12), (2008).
- ¹⁶A. Omrane, G. Särner, and M. Aldén, *Appl. Phys. B* **79**, 431 (2004).